

Large Dimeric Ligands with Favorable Pharmacokinetic Properties and Peroxisome Proliferator-Activated Receptor Agonist Activity in Vitro and in Vivo

Per Sauerberg,* Paul S. Bury, John P. Mogensen, Heinz-Josef Deussen, Ingrid Pettersson, Jan Fleckner, Jan Nehlin, Klaus S. Frederiksen, Tatjana Albrektsen, Nanni Din, L. Anders Svensson, Lars Ynddal, Erik M. Wulff, and Lone Jeppesen

Per Sauerberg, Novo Nordisk A/S, Novo Nordisk Park, 2760 Måløv, Denmark

Received May 22, 2003

Two potent nonselective, but PPAR α -preferring, PPAR agonists **5** and **6** were designed and synthesized in high yields. The concept of dimeric ligands in transcription factors was investigated by synthesizing and testing the corresponding dimers **7**, **8a**, and **8b** in PPAR transactivation assays. The three dimeric ligands all showed agonist activity on all three PPAR receptor subtypes, but with different profiles compared to the monomers **5** and **6**. Despite breaking all the “rule of five” criteria, the dimers had excellent oral bioavailability and pharmacokinetic properties, resulting in good in vivo efficacy in db/db mice. X-ray crystal structure and modeling experiments suggested that the dimers interacted with the AF-2 helix as well as with amino acid residues in the lipophilic pocket close to the receptor surface.

Introduction

Type 2 diabetes is a polygenic and progressive metabolic disorder characterized by insulin resistance, hyperglycaemia, hypertriglyceridaemia, and low plasma HDL-cholesterol. Untreated type 2 diabetes leads to several chronic diseases such as retinopathy, nephropathy, neuropathy, and cardiovascular diseases such as atherosclerosis, the latter leading to increased mortality.¹ The use of peroxisome proliferator-activated receptor γ (PPAR γ) activators, e.g. rosiglitazone and pioglitazone (glitazones), in the treatment of type 2 diabetes has been established over the last couple of years due to the abilities of these compounds to lower blood glucose and insulin levels and improve insulin sensitivity.^{2,3} Similarly, PPAR α activators, e.g. fenofibrate and clofibrate (fibrates), have been used clinically for more than two decades for their ability to lower plasma triglycerides and moderately raise HDL-cholesterol.⁴ Recently, very impressive increases in plasma HDL-cholesterol and decreases in plasma triglycerides in obese Rhesus monkeys treated with the PPAR δ selective agonist GW501516 have resulted in growing therapeutic interest in the third PPAR receptor.⁵

PPARs belong to the superfamily of nuclear hormone receptors including steroid receptor, thyroid receptor, retinoid receptor, and others. The PPAR receptors are ligand-dependent transcription factors, which upon ligand binding heterodimerize with the retinoid X receptor (RXR), recruit a coactivator, and modulate the transcription of the target genes after binding to specific peroxisome proliferator response elements.⁶

The present PPAR treatment of type 2 diabetes is still inadequate. Neither the fibrates nor the glitazones simultaneously lower triglycerides and increase HDL-c as well as lower blood glucose and improve insulin

sensitivity. To achieve this biological response several dual acting PPAR α,γ agonists (e.g. ragaglitazar/NNC61–0029,⁷ tesaglitazar/AZ242,⁸ and LY465608⁹) have been investigated in pre-clinical and clinical trials. Furthermore, triple PPAR α,γ,δ agonists have recently attracted interest, as this profile might further improve the clinical effects on the diabetic dyslipidemic parameters⁵ and also lower the PPAR γ -mediated side effects (e.g. oedema). The latter might be achieved because a 3–10 times lower PPAR γ dose was needed in rats and monkeys to obtain the same insulin-sensitizing effect when cotreated with a PPAR δ agonist.^{10,11} We have recently published on the identification of a group of triple PPAR α,γ,δ agonists¹² (**4**) using the dual PPAR α,γ activator¹³ (**1**) as a structural template (Figure 1). The goal of the present work was to extend the structural knowledge of this group of PPAR α,γ,δ agonists and to investigate if the concept of dimeric ligands could be applied to design PPAR agonists (Figure 1).

Thus, the present paper describes the design and synthesis of novel monomeric and dimeric ligands with full efficacy on all three PPAR receptors. Rat pharmacokinetic characterizations as well as in vivo evaluations in db/db mice show that these rather large ligands have surprisingly good in vivo properties making them possible drug candidates.

Chemistry

The biphenyl analogue **5** was made via a method analogous to the earlier published procedure for compounds **3** and **4**.¹² Commercially available 4-acetylbiphenyl was subjected to a Horner-Emmons reaction to give the *E*-butenoate isomer **9** as the only isolated product (Scheme 1). Diisobutyl aluminum hydride (DIBAL-H) reduction of the ester gave the desired alcohol **10** without reduction of the double bond. Alkylation of ethyl (*S*)-2-ethoxy-3-(4-hydroxyphenyl)propanoate¹⁴ with **10** under Mitsunobu conditions, followed

* Corresponding author. Telephone: +4544434858. Fax: +4544663939. e-mail: psa@novonordisk.com.

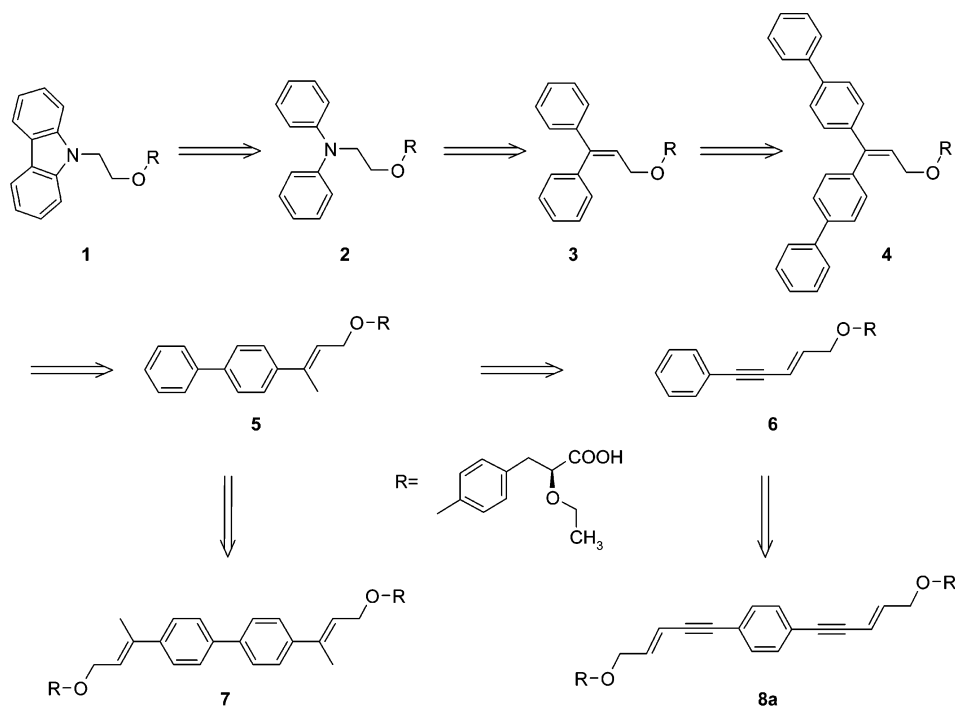
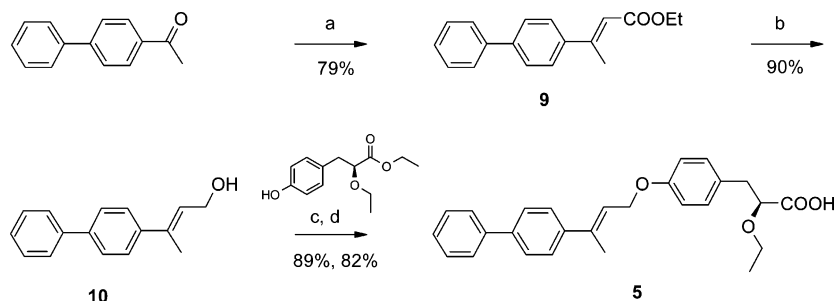


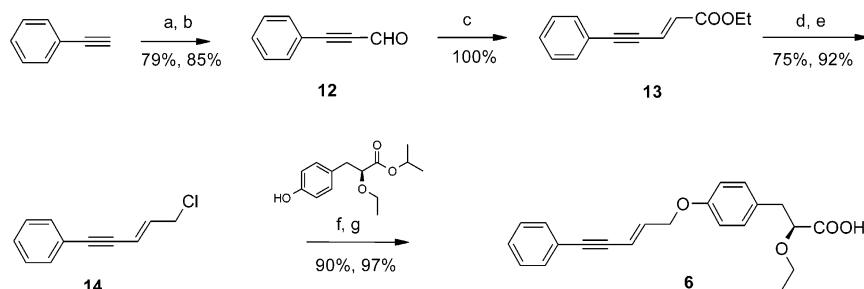
Figure 1. Graphical evolution of the project. The dual PPAR α,γ agonist **1** was structurally modified to the triple PPAR α,γ,δ agonist **4**.¹² Further modification gave the PPAR α -preferring triple PPAR α,γ,δ activators **5** and **6**. Applying the dimeric ligand design concept gave the triple PPAR α,γ,δ activators **7** and **8a**.

Scheme 1^a



^a (a) (i) Na, EtOH; (ii) (EtO)₂POCH₂COOEt, room temperature. (b) 1 M DIBAL-H in toluene, THF, -70 °C. (c) Ethyl (*S*)-2-ethoxy-3-(4-hydroxyphenyl)propanoate, P(Bu)₃, ADDP, THF, 0 °C to room temperature. (d) (i) 1 N NaOH, EtOH, room temperature; (ii) 1 N HCl.

Scheme 2^a

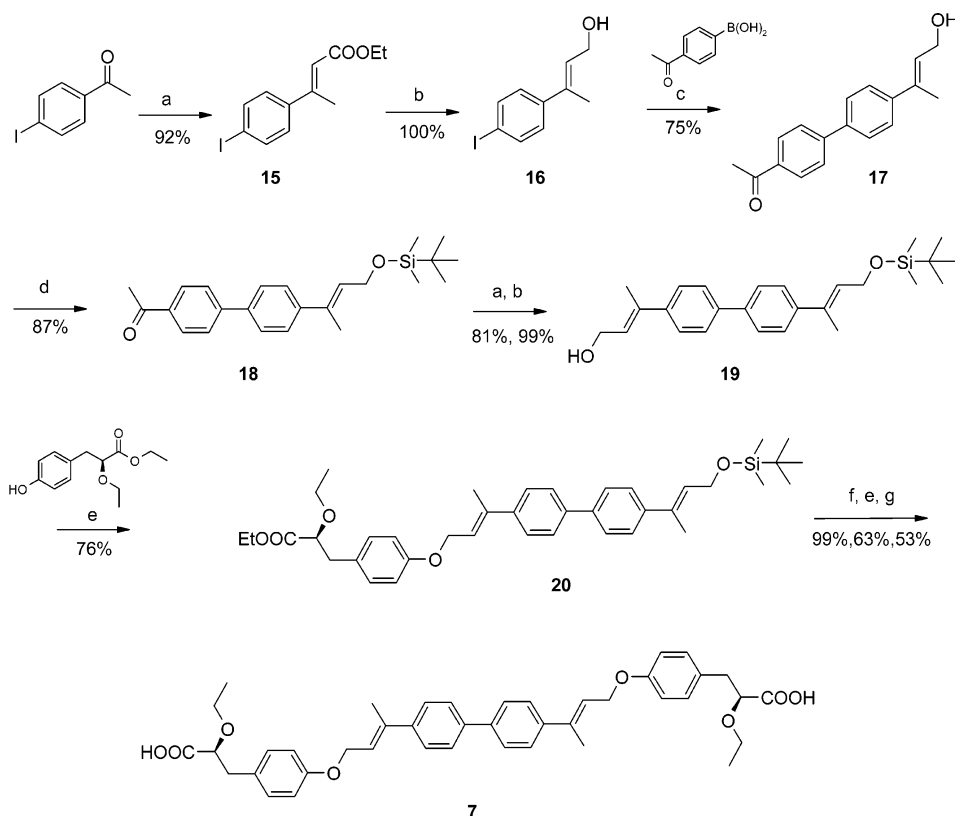


^a (a) CH(OEt)₃, ZnI₂, gradual heating with distillation (1–3 h). (b) 2 N H₂SO₄, heating with distillation. (c) (i) (EtO)₂POCH₂COOEt, NaOEt, toluene 1 h at room temperature; (ii) 2 N H₂SO₄. (d) DIBAL-H, toluene, -78 °C; (ii) 4 N HCl. (e) CH₃SO₂Cl, DMF, 65–70 °C. (f) Isopropyl (*S*)-2-ethoxy-3-(4-hydroxyphenyl)propanoate, K₂CO₃, KI, acetone, reflux. (g) 1 N NaOH, EtOH, 70 °C.

by hydrolysis of the ester to the carboxylic acid, gave the desired product **5** in 52% overall yield from 4-acetyl-biphenyl. As previously reported,¹³ coupling under Mitsunobu conditions and basic hydrolysis did not lead to racemization of the product.

The phenylacetylene analogue **6** was made in a slightly different way. The starting phenylacetylene aldehyde **12** was made according to a published Organic Synthesis procedure¹⁵ (Scheme 2). The aldehyde **12** was

then subjected to a similar Horner–Emmons reaction to give the α,β -unsaturated ester **13**.¹⁶ DIBAL-H reduction of the ester gave the alcohol¹⁷ as described above for compound **5**. However, the obtained alcohol was not subjected to a Mitsunobu reaction, as this tended to give lower yields and a difficult workup. Instead, the alcohol was converted to the allylic chloride **14** in high yield via the iminium salt generated in situ from methanesulfonyl chloride in DMF.¹⁸ Alkylation of the phenol

Scheme 3^a

^a (a) (i) Na, EtOH; (ii) (EtO)₂POCH₂COOEt. (b) 1 M DIBAL-H in toluene, THF. (c) (i) Pd(PPh₃)₄, 2 M Na₂CO₃, DME, room temperature; (ii) 4-acetylphenylboronic acid, 65 °C to room temperature. (d) Imidazole, TBDMSCl, CH₂Cl₂, room temperature. (e) Ethyl (*S*)-2-ethoxy-3-(4-hydroxy-phenyl)propanoate, P(Bu)₃, ADDP, THF, 0 °C to room temperature. (f) 1.1 M N(Bu)₄F, THF, room temperature. (g) 1 N NaOH, EtOH.

derivative with **14** in acetone under standard conditions gave the desired ester in high yield. Alkaline hydrolysis of the ester gave the target molecule **6** in 40% yield over the seven steps.

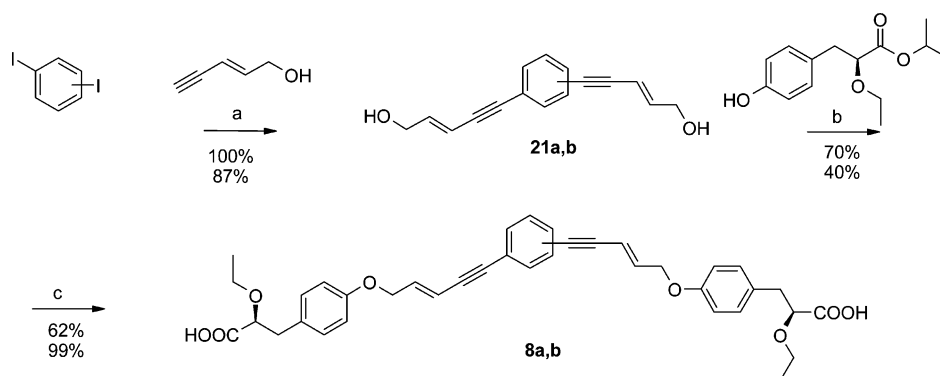
The strategy for synthesizing the dimer **7** was originally very similar to the synthesis of compound **5**. The intention was to make the dialcohol (unprotected **19**) and react this with ethyl (*S*)-2-ethoxy-3-(4-hydroxy-phenyl)propanoate to directly give the diester of **7**. This strategy failed, however, as the dialcohol turned out to be unstable. The alternative and successful method is outlined in Scheme 3. 4-Iodoacetophenone was reacted with triethylphosphonoacetate followed by a DIBAL-H reduction to give the intermediate **16**. Again, the Horner-Emmons reaction gave **15** exclusively as the *E* isomer, which was confirmed by NOE NMR experiments. The iodophenyl alcohol **16** was coupled with 4-acetylphenylboronic acid using Suzuki conditions to give **17**. As the dialcohol was unstable, the hydroxyl functionality in **17** was protected as the *tert*-butyldimethylsilyl ether (**18**) before the ketone was subjected to Horner-Emmons condensation and reduction to give the mono-protected dialcohol **19**. Alkylation of ethyl (*S*)-2-ethoxy-3-(4-hydroxy-phenyl)propanoate under Mitsunobu conditions with the free alcohol of **19** gave **20**. After fluoride de-protection and repeated Mitsunobu coupling of the second alcohol group, the ester of the desired dimer was obtained. Alkaline hydrolysis of the esters gave the target molecule **7** in moderate overall yield.

The dimeric compounds **8a** and **8b** were easily obtained using cross-coupling conditions between the

commercially available reagents 1,3- and 1,4-diiodobenzene and 2-penten-4-yn-1-ol, as shown in Scheme 4. The palladium and copper(I) assisted reactions gave the dialcohols **21a** and **21b** in high yields. These dialcohols, **21a** and **b**, could, contrary to the dialcohol described above, be reacted under Mitsunobu conditions to give the esters of the target dimers. Standard hydrolysis gave **8a** and **8b**.

Results and Discussion

We have recently published on our design of triple PPAR α,γ,δ activators starting from a dual PPAR α,γ agonist (Figure 1, compounds **1–4**).¹² The aim of the present work was to extend the structural knowledge of this type of compounds and to investigate if the dimeric approach could be applied to PPAR ligands. As in our previous research, the *in vitro* transactivation assays with the ligand binding domains (LBDs) of each of the three human PPAR (hPPAR) receptor subtypes were used as the primary screening tools in that effort. Further, to avoid misinterpretations of the animal data due to the known possible species differences with PPAR α ligands, the compounds were also tested in the rat PPAR α (rPPAR α) transactivation assay. To compare the efficacy of compounds from test to test WY 14643, rosiglitazone and carbacyclin were used as reference agonists in the hPPAR α , hPPAR γ , and hPPAR δ assays, respectively. The importance of high and sustained plasma exposure for good *in vivo* PPAR efficacy¹³ prompted us to subject interesting compounds

Scheme 4^a

^a (a) (i) CuI, Pd(PPh₃)₄, NH(Pr)₂, room temperature; (ii) 2-penten-4-yn-1-ol, 60°C. (b) isopropyl (S)-2-ethoxy-3-(4-hydroxy-phenyl)propanoate, P(Bu)₃, ADDP, THF, room temperature. (c) (i) 1 N NaOH, EtOH, 80 °C; (ii) 1 N HCl.

to pharmacokinetic evaluation early in the characterization process.

The triple PPAR α,γ,δ agonist **4**, Figure 1, (α : 77%, EC₅₀ = 1.1 μ M; γ : 101%, 0.3 μ M; δ : 265%, 0.5 μ M)¹² was used as the structural lead. Replacement of one of the biphenyl groups in **4** with a methyl group gave compound **5**, which retained full triple PPAR α,γ,δ agonist activity, although with lower PPAR γ and PPAR δ potencies (Table 1). However, the rat pharmacokinetic properties of **5** were excellent, with high plasma exposure, high oral bioavailability, low clearance, and the resulting long half-life after oral administration (Table 2). These properties resulted in a potent and efficacious lowering of plasma triglycerides, blood glucose, and plasma insulin levels in male db/db mice treated orally once a day for 7 days (Table 3). The animals were dosed for a further 2 days, whereupon an oral glucose test (OGTT) was performed. The reduction of the blood glucose area under curve (AUC_{glu}) was considered to be a more direct measure of improved insulin sensitivity. Compound **5** also reduced the AUC_{glu} potently and more efficaciously than rosiglitazone and pioglitazone (Table 3). The db/db mice were considered an *in vivo* model for primarily PPAR γ activation since PPAR α treatment only had marginal effects (Table 3) and in the closely related ob/ob mice model the antihyperglycemic activity of PPAR γ agonists correlated with their *in vitro* PPAR γ activity.¹⁹ Despite lower *in vitro* PPAR γ potency, the treatment effects of **5** were more pronounced than with the two PPAR γ reference compounds rosiglitazone and pioglitazone (as well as with the PPAR α compounds WY 14643 and fenofibrate). These improved effects could be due to the good pharmacokinetic properties, the triple PPAR α,γ,δ activation or a combination of the two.

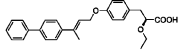
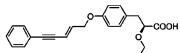
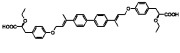
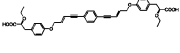
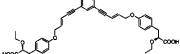
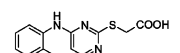
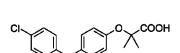
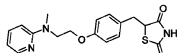
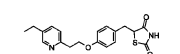
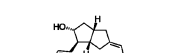
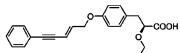
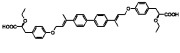
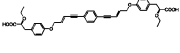
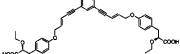
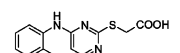
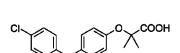
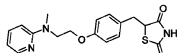
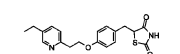
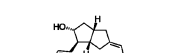
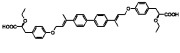
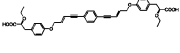
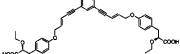
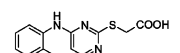
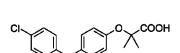
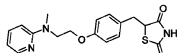
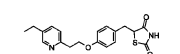
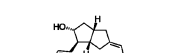
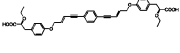
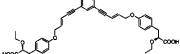
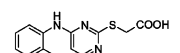
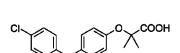
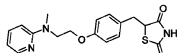
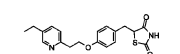
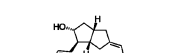
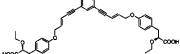
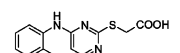
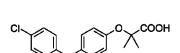
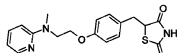
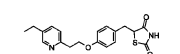
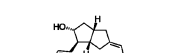
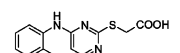
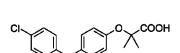
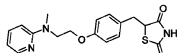
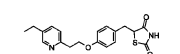
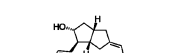
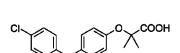
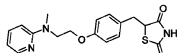
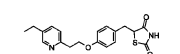
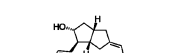
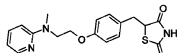
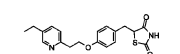
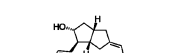
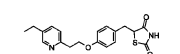
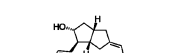
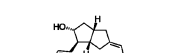
Further, replacing one of the phenyl groups in **5** with an acetylene group gave compound **6**, which was 10 times more potent on PPAR α than **5**, whereas the potency and efficacy of PPAR γ and PPAR δ were basically unchanged (Table 1). The pharmacokinetic properties of **6** were comparable to those of **5**, although the plasma half-life was considerably shorter (Table 2). The effects of **6** in db/db mice were also slightly less potent and efficacious than obtained with **5**, but the effects were still more efficacious than seen with both rosiglitazone and pioglitazone (Table 3).

Structural information on the binding pockets of all the PPAR receptor subtypes, all showing large binding cavities, prompted us to investigate the possibility of

designing dimeric ligands. Dimeric or bivalent ligands have primarily been used in the design of G-protein-coupled receptor antagonists and uptake inhibitors, but also a few agonists have been reported. Improved receptor subtype selectivity and/or improved potency have been reported for some of these dimeric ligands over their monomeric leads (for a review of this area see S. Halazy²⁰). Dimeric ligands are usually defined as molecules containing two recognition units linked covalently through either a common group or through a spacer. We have earlier reported on the successful design of potent and receptor subtype selective muscarinic agonists employing the dimeric ligand design through a common group,²¹ and this approach was consequently pursued. Several papers have demonstrated that hydrogen bond interactions between the AF-2 helix in the PPAR receptor protein and the carboxylic acid/thiazolidinedione moiety in the ligand are essential for agonist activity.^{22,23} Dimeric ligands coupled through the lipophilic end of **5** and **6** giving the bivalent molecules **7** and **8** were therefore designed (Figure 1). Interestingly, all three compounds, **7**, **8a**, and **8b**, were full agonists on the three PPAR receptor subtypes, but they had different potency ratios compared to **5** and **6** (Table 1). For instance, **7** and **8a** were more potent on PPAR γ than on PPAR α and PPAR δ , whereas **5** and **6** were most potent on PPAR α . Further, all the test compounds (**5**–**8**) had higher potency for the hPPAR α than for the rPPAR α . None of the compounds had transactivation activity on the heterodimeric partner of PPAR, the hRXR α receptor (data not shown). This demonstrates for the first time that the dimeric approach can be utilized to change the receptor subtype selectivity of PPAR ligands *in vitro*.

The synthesized dimeric agonists were, however, quite large with molecular weights above 500 g/mol, mLogP above 4.15, cLogP above 5, the number of rotatable bonds above 20, and polar surface areas (PSA) above 120 Å² (Table 4), all characteristics traditionally indicating poor pharmacokinetic properties.^{24,25} Surprisingly, all three dimeric ligands, but especially **7** and **8a**, exhibited excellent pharmacokinetic properties with extremely high maximal plasma concentrations (C_{max}), very high oral bioavailabilities (F_{po}), very low plasma clearances (CL), very low volume of distributions (V_{ss}), and the desired long plasma half-lives ($T_{1/2(po)}$, Table 2). The reason for these excellent pharmacokinetic properties was not investigated further, but we speculate that

Table 1. In Vitro hPPAR α , rPPAR α , hPPAR γ , and hPPAR δ Transactivation of Test and Reference Compounds^a

Compd	Structure	In vitro transactivation																																																																																									
		hPPAR α rPPAR α		hPPAR γ		hPPAR δ																																																																																					
		EC ₅₀ ±SD, μM	% max±SD ^b	EC ₅₀ ±SD, μM	% max±SD ^c	EC ₅₀ ±SD, μM	% max±SD ^d																																																																																				
5		0.49±0.30	158±48	2.03±1.83	118±17	9.55±2.87	235±13																																																																																				
		11.1±2.0	166±9					6		0.067±0.030	123±36	1.13±0.33	98±10	6.90±1.08	173±16	0.70±0.0	112±2	7		6.69±2.19	247±49	0.32±0.20	162±15	2.08±1.38	314±63	19.9±1.3	203±79	8a		0.71±0.32	173±49	0.11±0.02	103±11	2.17±1.60	238±51	6.30±0.10	210±16	8b		0.30±0.044	193±50	1.65±0.025	102±6	10.50±2.27	112±30	4.60±2.30	109±47	WY 14643		12.6±1.1	100	29.3±4.3	22±3	NC	6±6	2.10±0.50	100	fenofibric acid		32.05±9.49	265±34	NC	8±3	NC	1±0.1	131.3±23.2	331±70	rosi- glitazone		4.1±1.4	43±8	0.16±0.015	100	NC	7±5	-	22±17	pioglitazone		6.68±2.33	58±20	0.97±0.14	91±7	NC	1±0	-	4±1	carba- cyclin		0.96±0.71	79±35
6		0.067±0.030	123±36	1.13±0.33	98±10	6.90±1.08	173±16																																																																																				
		0.70±0.0	112±2					7		6.69±2.19	247±49	0.32±0.20	162±15	2.08±1.38	314±63	19.9±1.3	203±79	8a		0.71±0.32	173±49	0.11±0.02	103±11	2.17±1.60	238±51	6.30±0.10	210±16	8b		0.30±0.044	193±50	1.65±0.025	102±6	10.50±2.27	112±30	4.60±2.30	109±47	WY 14643		12.6±1.1	100	29.3±4.3	22±3	NC	6±6	2.10±0.50	100	fenofibric acid		32.05±9.49	265±34	NC	8±3	NC	1±0.1	131.3±23.2	331±70	rosi- glitazone		4.1±1.4	43±8	0.16±0.015	100	NC	7±5	-	22±17	pioglitazone		6.68±2.33	58±20	0.97±0.14	91±7	NC	1±0	-	4±1	carba- cyclin		0.96±0.71	79±35	7.91±3.13	24±6	1.88±0.68	100	-	15±6				
7		6.69±2.19	247±49	0.32±0.20	162±15	2.08±1.38	314±63																																																																																				
		19.9±1.3	203±79					8a		0.71±0.32	173±49	0.11±0.02	103±11	2.17±1.60	238±51	6.30±0.10	210±16	8b		0.30±0.044	193±50	1.65±0.025	102±6	10.50±2.27	112±30	4.60±2.30	109±47	WY 14643		12.6±1.1	100	29.3±4.3	22±3	NC	6±6	2.10±0.50	100	fenofibric acid		32.05±9.49	265±34	NC	8±3	NC	1±0.1	131.3±23.2	331±70	rosi- glitazone		4.1±1.4	43±8	0.16±0.015	100	NC	7±5	-	22±17	pioglitazone		6.68±2.33	58±20	0.97±0.14	91±7	NC	1±0	-	4±1	carba- cyclin		0.96±0.71	79±35	7.91±3.13	24±6	1.88±0.68	100	-	15±6														
8a		0.71±0.32	173±49	0.11±0.02	103±11	2.17±1.60	238±51																																																																																				
		6.30±0.10	210±16					8b		0.30±0.044	193±50	1.65±0.025	102±6	10.50±2.27	112±30	4.60±2.30	109±47	WY 14643		12.6±1.1	100	29.3±4.3	22±3	NC	6±6	2.10±0.50	100	fenofibric acid		32.05±9.49	265±34	NC	8±3	NC	1±0.1	131.3±23.2	331±70	rosi- glitazone		4.1±1.4	43±8	0.16±0.015	100	NC	7±5	-	22±17	pioglitazone		6.68±2.33	58±20	0.97±0.14	91±7	NC	1±0	-	4±1	carba- cyclin		0.96±0.71	79±35	7.91±3.13	24±6	1.88±0.68	100	-	15±6																								
8b		0.30±0.044	193±50	1.65±0.025	102±6	10.50±2.27	112±30																																																																																				
		4.60±2.30	109±47					WY 14643		12.6±1.1	100	29.3±4.3	22±3	NC	6±6	2.10±0.50	100	fenofibric acid		32.05±9.49	265±34	NC	8±3	NC	1±0.1	131.3±23.2	331±70	rosi- glitazone		4.1±1.4	43±8	0.16±0.015	100	NC	7±5	-	22±17	pioglitazone		6.68±2.33	58±20	0.97±0.14	91±7	NC	1±0	-	4±1	carba- cyclin		0.96±0.71	79±35	7.91±3.13	24±6	1.88±0.68	100	-	15±6																																		
WY 14643		12.6±1.1	100	29.3±4.3	22±3	NC	6±6																																																																																				
		2.10±0.50	100					fenofibric acid		32.05±9.49	265±34	NC	8±3	NC	1±0.1	131.3±23.2	331±70	rosi- glitazone		4.1±1.4	43±8	0.16±0.015	100	NC	7±5	-	22±17	pioglitazone		6.68±2.33	58±20	0.97±0.14	91±7	NC	1±0	-	4±1	carba- cyclin		0.96±0.71	79±35	7.91±3.13	24±6	1.88±0.68	100	-	15±6																																												
fenofibric acid		32.05±9.49	265±34	NC	8±3	NC	1±0.1																																																																																				
		131.3±23.2	331±70					rosi- glitazone		4.1±1.4	43±8	0.16±0.015	100	NC	7±5	-	22±17	pioglitazone		6.68±2.33	58±20	0.97±0.14	91±7	NC	1±0	-	4±1	carba- cyclin		0.96±0.71	79±35	7.91±3.13	24±6	1.88±0.68	100	-	15±6																																																						
rosi- glitazone		4.1±1.4	43±8	0.16±0.015	100	NC	7±5																																																																																				
		-	22±17					pioglitazone		6.68±2.33	58±20	0.97±0.14	91±7	NC	1±0	-	4±1	carba- cyclin		0.96±0.71	79±35	7.91±3.13	24±6	1.88±0.68	100	-	15±6																																																																
pioglitazone		6.68±2.33	58±20	0.97±0.14	91±7	NC	1±0																																																																																				
		-	4±1					carba- cyclin		0.96±0.71	79±35	7.91±3.13	24±6	1.88±0.68	100	-	15±6																																																																										
carba- cyclin		0.96±0.71	79±35	7.91±3.13	24±6	1.88±0.68	100																																																																																				
		-	15±6																																																																																								

^a Compounds were tested in at least three separate experiments in five concentrations ranging from 0.01 to 30 μM. EC₅₀'s were not calculated (NC) for compounds producing transactivation lower than 25% at 30 μM. ^bFold activation relative to maximum activation obtained with WY14643 (approximately 20-fold for human and approximately 75-fold for rat corresponded to 100%), with ^crosiglitazone (approximately 120-fold corresponded to 100%) and with ^dcarbacyclin (approximately 250-fold corresponded to 100%).

the high oral bioavailability may be due to active transporters (e.g. the Oatp in rats²⁶) and/or enterohepatic recirculation, as earlier reported for PPAR ligands.¹³ The impressive in vivo effects in db/db mice confirmed the tested dimeric agonists as being possible drug candidates (Table 3 and Figures 2a and 2b).

In an attempt to explain the altered pharmacological profiles of the dimeric ligands compared to their monomeric leads, a crystal of LBD-hPPAR γ receptor was soaked in a solution containing **7**. The X-ray structure showed that one-half of the ligand, the half closer to the AF-2 helix, had well-defined electron densities, whereas

Table 2. Single Dose Rat Pharmacokinetics after iv and po Administration

compound	single dose rat pharmacokinetic					
	C_{\max} po, ^a ng/mL	AUC po, ^b (ng × min)/mL	F_{po} , ^c %	CL, ^d mL/min/kg	V_{ss} , ^e L/kg	$T_{1/2}$ po, ^f min
5 ^g	9249	6974138	100	0.49	0.16	213
6, arg	4570	3732353	89	0.54	0.14	122
7	23220	587145	58	0.04	0.08	>400
8a	27780	6647520	100	0.10	0.04	>360
8b	7214	5096888	63	0.23	0.16	402
rosiglitazone	4420	873922	83	2.10	0.38	182

Rats were given either a single dose iv (1.1 mg/kg) ($n = 8$) or a single dose po (2.2 mg/kg) ($n = 8$) of each of the test compounds. At each of the time points (5, 15, 30, 60, 90, 120, 240, and 360 min), one animal was sacrificed and blood samples were analyzed for compound plasma concentration. ^aMaximum plasma concentration after oral dosing. ^bEstimated area under the plasma concentration–time curve after oral dosing. ^cOral bioavailability. ^dClearance. ^eVolume of distribution during steady state. ^fOral half-life. ^gAdministered 1.74 mg/kg iv and 3.42 mg/kg po.

Table 3. In Vivo Effects in Male db/db Mice after Oral Treatment for 7–9 Days

compound	in vivo effects in db/db mice after 7–9 days oral treatment							
	BG, ^a ED ₅₀ , mg/kg	BG, % max reduction	TG, ^b ED ₅₀ , mg/kg	TG, % max reduction	insulin, ED ₅₀ , mg/kg	insulin, % max reduction	AUCglu, ^c ED ₅₀ , mg/kg	AUCglu, % max reduction
5	0.2 ± 0.8	53 ± 2	0.3 ± 0.6	65 ± 1	0.2 ± 0.9	95 ± 1	0.3 ± 0.6	50 ± 5
6, arg	0.4 ± 0.7	54 ± 4	0.4 ± 0.6	57 ± 3	1.0 ± 1.5	92 ± 1	1.2 ± 0.7	45 ± 3
7	0.2 ± 0.9	40 ± 7	0.3 ± 0.7	60 ± 3	0.2 ± 0.7	91 ± 2	0.4 ± 0.6	53 ± 5
8a	0.4 ± 0.6	55 ± 1	0.2 ± 1.1	56 ± 3	0.4 ± 0.6	90 ± 3	0.9 ± 0.6	52 ± 2
8b	0.9 ± 0.6	54 ± 10	0.1 ± 0.8	46 ± 4	0.6 ± 1.1	86 ± 2	0.5 ± 0.6	60 ± 6
WY 14643	2.2 ± 1.0	36 ± 8	3.0 ± 0.5	32 ± 2	15 ± 0.9	45 ± 16	4.7 ± 1.0	13 ± 12
fenofibrate	>300	10 ± 3	>300	20 ± 6	191 ± 22	32 ± 16	>300	0 ± 6
rosiglitazone	0.9 ± 0.6	35 ± 7	0.1 ± 1.0	58 ± 2	0.1 ± 1.3	43 ± 9	0.8 ± 0.6	16 ± 9
pioglitazone	2.6 ± 0.2	53 ± 3	27 ± 0.6	21 ± 5	15 ± 1.0	54 ± 10	12 ± 0.8	39 ± 8

Male db/db mice ($n = 6$) were treated once a day by oral gavage for 9 days. Compounds **5**, **6**, **7**, and **8a** were tested at the doses 0.3, 1, 3, and 10 mg/kg/day, **8b** at 0.1, 0.3, 1, and 3 mg/kg/day, WY 14643 at 1, 3, 10, and 30 mg/kg/day, fenofibrate at 10, 30, 100, and 300 mg/kg/day, rosiglitazone at 0.2, 0.6, 2, and 6 mg/kg/day, and pioglitazone at 3, 10, 30, and 100 mg/kg/day. ED₅₀ values were calculated via nonlinear regression using GraphPad PRISM 3.02 and are expressed as mean ± SEM. % max reduction is the maximum achieved reduction relative to vehicle treated control group, ± SEM. ^aNonfasting blood glucose after 7 days treatment. ^bNonfasting triglycerides after 7 days treatment. ^cArea under blood glucose time curve after OGTT on the 9th day of treatment.

Table 4. Calculated Physical/Chemical Properties of Test and Reference Compounds

compound	MW ^a g/mol	mLogP	cLogP ^b	HBdonors ^c	HBaccep ^d	rotatable bonds ^e	PSA, ^f Å ²
5	416.5	4.50	6.66	1	4	13	64.14
6	350.4	3.87	4.53	1	4	12	64.09
7	678.8	4.89	9.30	2	8	25	128.28
8a	622.7	4.81	6.91	2	8	24	128.2
8b	622.7	4.81	6.91	2	8	24	128.2
fenofibrate	360.8	4.27	5.89	0	4	11	51.98
rosiglitazone	357.4	1.91	3.02	1	6	8	77.79

^aMolecular weight. ^bCalculated by Sybyl 6.6. ^cNumber of hydrogen bond donors. ^dNumber of hydrogen bond acceptors. ^eNumber of rotatable bonds of nonterminal heavy (i.e., non-hydrogen) atoms. ^fPolar surface area, calculated by SAVOL 3.7.

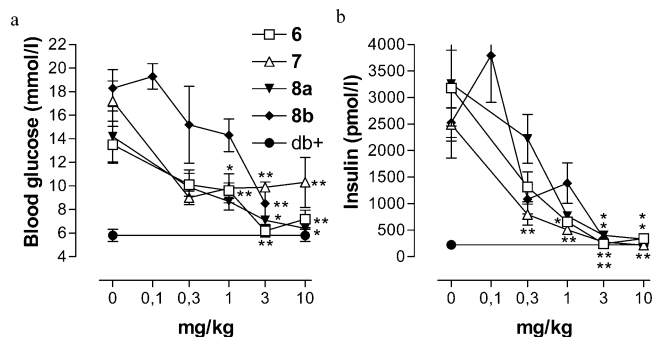


Figure 2. Dose-related reduction of the nonfasted blood glucose (a) and of the nonfasted plasma insulin (b) in male db/db mice ($n = 6$) treated for 7 days with **6**, **7**, **8a**, and **8b** orally once a day. Values are expressed as mean ± SEM. * represents $P < 0.05$, ** $P < 0.01$ using one-way ANOVA and Dunetts multiple comparison test.

the opposite half could not be unambiguously positioned, indicating high flexibility (Figure 3). The well-defined part of **7** superimposed well with previously published (S)-2-ethoxy-3-(4-substituted-phenyl)propionic acid

derivatives¹³ and made the earlier reported hydrogen bond interactions.^{22,23} Docking experiments of **7** into the published structure of the heterodimer of the hRXR α :hPPAR γ LBDs respectively bound with 9-*cis*-retinoic acid and GI262570, and coactivator peptides²⁷ were performed to investigate possible interactions of the flexible end of the ligand. To validate the predicted binding mode, GI262570 was first docked into the binding pocket. FlexX gave solutions with CScore equal to five and 1.2 as the root-mean-square (rms) values to the crystallized ligand.²⁷ Docking of **7** gave solutions with high CScore values and a binding mode which for one part of the ligand occupied the same pocket as GI262570 and for the other end of **7** a part of the binding pocket reported to be occupied by the partial agonist GW0072²⁸ (Figure 3). In the predicted binding mode a hydrogen bond interaction between the carboxylic acid group in **7** and Q273 was observed. As the docking was performed with a rigid protein which is not a correct description of ligand binding, interactions between the carboxylic acid group and other amino acids in this part

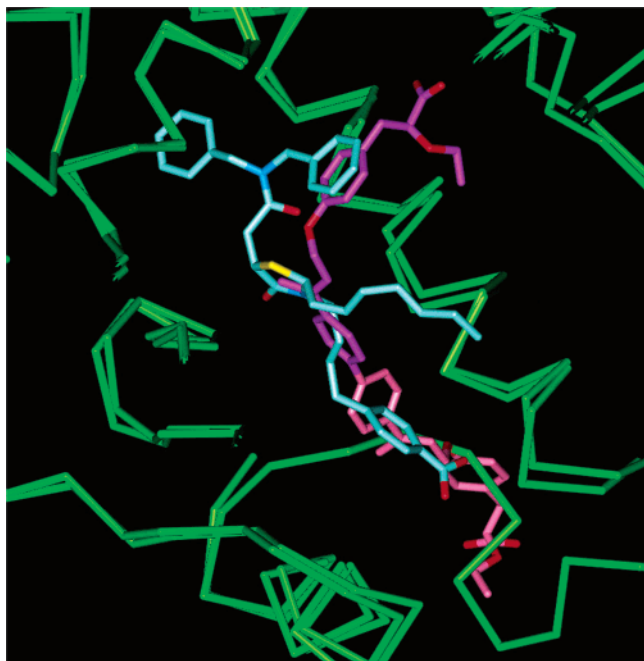


Figure 3. Crystal structure of the ligand binding domain of the hPPAR γ receptor (green) soaked with the dimeric ligand **7** (light and dark magenta) and superimposed with the crystal structure of the partial PPAR γ agonist GW0072 (light blue).²⁸ The light magenta part of **7** depicts the less well-defined part of the crystal structure.

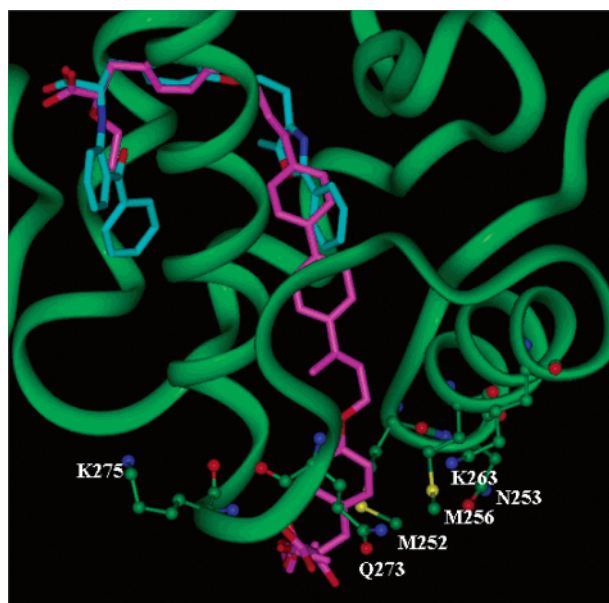


Figure 4. Superimposition of the ligand binding domain of the hPPAR γ receptor (green) crystallized with GI262570 (cyan) in the hRXR α :hPPAR γ :SRC-1 receptor complex²⁷ and the four most diverse FlexX docking solutions of the dimeric ligand **7** (magenta). The amino acids closest to the carboxylic acid in **7** (the one not interacting with the AF-2 helix) are shown as ball-and-stick. Hydrogen bond interaction was observed between the carboxylic acid in **7** and the NH₂ group in the glutamine Q273.

of the binding pocket cannot be ruled out. The amino acids with hydrophilic side chains within 15 Å from the carboxylic acid group in **7** are shown in ball-and-stick in Figure 4, and interactions between the carboxylic acid group in **7** and one of these amino acids could be possible. The alignment of the amino acids in the hPPAR α , hPPAR γ , and hPPAR δ receptors in this pocket

is shown in Figure 5. In this alignment it can be seen that there are differences in the amino acid sequences between the three receptors which might affect the interactions between the receptors and the ligand and give rise to a change in the $\alpha/\gamma/\delta$ profile for the dimeric compounds. Due to the flexibility of the receptors, a situation in which the carboxylic acid group introduces different shapes for the different receptors cannot be rejected. The difference in amino acid sequences and the possibility of the binding pocket to adopt different shapes for the hPPAR α , hPPAR γ , and hPPAR δ receptors are possible explanations of the change in receptor subtype profile going from the monomeric to the dimeric ligands.

In conclusion, the PPAR agonists **5** and **6** as well as their dimeric analogues **7**, **8a**, and **8b** were designed and synthesized in good overall yields. In vitro PPAR α , γ , and δ transactivation data showed the designed ligands to be potent PPAR agonists exhibiting different PPAR receptor subtype profiles. X-ray crystal structure and modeling experiments suggested that part of the receptor subtype profile could be due to interactions with amino acids residing close to the receptor surface. Rat pharmacokinetic evaluations revealed surprisingly favorable oral absorption and plasma half-lives of these quite large bivalent ligands. The in vivo db/db mice efficacy data confirmed that the evaluated dimeric PPAR ligands might be suitable drug candidates, further suggesting that the principle of dimeric ligands could be applied more broadly than seen until now.²⁹

Experimental Section

Chemistry. Melting points were determined on a Büchi capillary melting point apparatus and are uncorrected. ¹H NMR spectra were recorded at either 200 MHz on a Bruker Advance DPX 200 instrument, at 300 MHz on a Bruker Advance DRX 300 instrument, or at 400 MHz on a Bruker Advance DRX 400 instrument, and mass spectra were recorded on a Finnigan 5100 mass spectrometer. Capillary electrophoresis (CE) was run on an Agilent Technologies capillary electrophoresis instrument. Capillary: Agilent part no. 61600-62232, 72 cm, 50 μ m i.d., bubble cell. Column chromatography was performed on silica gel 60 (70-230 mesh, ASTM, Merck). Elemental analyses were performed by the Novo Nordisk Microanalytical Laboratory, Denmark, and were within $\pm 0.4\%$ of the calculated values.

Ethyl (E)-3-Biphenyl-4-ylbut-2-enoate, 9. Sodium (6.0 g, 255 mmol) was added to ethanol (700 mL) at 20 °C and the mixture stirred until the metal had fully reacted. Triethyl phosphonoacetate (57.12 g, 255 mmol) was added, the mixture stirred for 5 min, then 4-acetylbiphenyl (25.0 g, 127 mmol) added to the stirred solution. The mixture was stirred at room temperature for 24 h, the resulting suspension filtered, and the crystals washed with ethanol (100 mL) to give the title compound as white crystals in 26.6 g (79%) yield. ¹H NMR (CDCl₃) δ 1.32 (3H, t, J = 7 Hz), 2.62 (3H, d, J = 1.5 Hz), 4.21 (2H, q, J = 7 Hz), 6.20 (1H, d, J = 1.5 Hz), 7.31-7.65 (9H, m).

(E)-3-Biphenyl-4-ylbut-2-en-1-ol, 10. A 1 M solution of DIBAL-H in toluene (255 mL, 255 mmol) was added dropwise at -70 °C over 1 h to a stirred solution of **9** (15.0 g, 56.3 mmol) in dry THF (200 mL), and the mixture stirred for 90 min. Saturated aqueous ammonium chloride was carefully added to quench the reaction, and the resulting mixture was extracted with ethyl acetate (250 mL). The organic phases were washed with brine, dried (Na₂SO₄), and evaporated. The residue was crystallized from ethanol to give the title compound as colorless crystals in 11.3 g (90%) yield. ¹H NMR (CDCl₃) δ 1.40 (1H, br s), 2.12 (3H, d, J = 1.5 Hz), 4.40 (2H, d, J = 6 Hz), 6.05 (1H, dt, J = 5 Hz, 1.5 Hz), 7.35-7.70 (9H, m).

PPAR α	M	E	T	L	C	M	A	E	-	K	T	L	V	A	K	L	V	A	N	G	I	Q	N	K
PPAR δ	I	E	T	L	W	Q	A	E	K	G	L	V	W	K	Q	L	V	N	G	L	P	P	Y	K
PPAR γ	M	N	S	L	M	M	G	E	D	K	I	K	F	K	H	I	T	P	L	Q	E	Q	S	K
	252	253			256							263									273	275		

Figure 5. Alignment of the amino acids close to the receptor surface in the hPPAR α , hPPAR γ , and hPPAR δ receptors.

Ethyl (*E*)-(S)-3-[4-(3-Biphenyl-4-ylbut-2-enyloxy)phenyl]-2-ethoxypropanoate. To a solution of **10** (4.0 g, 17.8 mmol) and ethyl (*S*)-2-ethoxy-3-(4-hydroxyphenyl)propanoate¹⁴ (4.2 g, 17.8 mmol) in dry THF (500 mL) were added a solution of tributylphosphine (7.2 g, 35.7 mmol) and azodicarboxylic dipiperidine (9.0 g, 35.7 mmol) in dry THF (150 mL) at 0 °C. The reaction mixture was allowed to warm to room temperature and stirred for 24 h. The resulting mixture was evaporated in vacuo and the residue purified by column chromatography using ethyl acetate:*n*-heptane (1:5) as eluent to give the title compound as an oil in 7.0 g (89%) yield. ¹H NMR (CDCl₃) δ 1.17 (3H, t, *J* = 7 Hz), 1.22 (3H, t, *J* = 7 Hz), 2.17 (3H, d, *J* = 2 Hz), 2.96 (2H, d, *J* = 7 Hz), 3.29–3.37 (1H, m), 3.54–3.61 (1H, m), 3.97 (1H, t, *J* = 7 Hz), 4.17 (2H, q, *J* = 7.5), 4.70 (2H, d, *J* = 6 Hz), 6.11 (1H, m), 6.88 (2H, d, *J* = 8 Hz), 7.17 (2H, d, *J* = 8 Hz), 7.25–7.63 (9H, m).

(*E*)-(S)-3-[4-(3-Biphenyl-4-ylbut-2-enyloxy)phenyl]-2-ethoxypropanoic Acid, 5. Sodium hydroxide (1 M, 33 mL, 33 mmol) was added to a solution of ethyl (*E*)-(S)-3-[4-(3-biphenyl-4-ylbut-2-enyloxy)phenyl]-2-ethoxypropanoate (5.0 g, 11.0 mmol) in ethanol (60 mL) and the mixture stirred at 20 °C for 5 h. The reaction was acidified with 1 N hydrochloric acid (31 mL), and the resulting precipitate was collected by filtration and dried to give the title compound a white solid in 3.7 g (82%) yield. ee > 93% (CE). ¹H NMR (CDCl₃) δ 1.19 (3H, t, *J* = 7 Hz), 2.63 (3H, d, *J* = 7 Hz), 2.93 (1H, dd, *J* = 14 Hz, 7 Hz), 3.10 (1H, dd, *J* = 14 Hz, 5 Hz), 3.40–3.65 (2H, m), 4.10 (2H, q, *J* = 7 Hz), 4.72 (2H, d, *J* = 7 Hz), 6.10 (1H, dt, *J* = 5 Hz, 1 Hz), 6.90 (2H, d, *J* = 8 Hz), 7.20 (2H, d, *J* = 8 Hz), 7.35–7.60 (9H, m). Mp 118–120 °C. Anal. (C₂₇H₂₈O₄) C, H, N.

(*E*)-5-Chloropent-3-en-1-ynylbenzene, 14. To a solution of (*E*)-5-phenylbut-2-en-1-yn-1-ol¹⁷ (53.0 g, 335 mmol) in DMF (150 mL) was added methanesulfonyl chloride (42.2 g, 368 mmol) dropwise with stirring. The temperature rose to 60–70 °C, and the reaction mixture was kept at that temperature for 1 h after complete addition. The reaction mixture was allowed to cool to ambient temperature followed by the addition of water (150 mL). The mixture was then extracted with toluene (2 \times 100 mL), and the combined organic phases were washed with water (2 \times 100 mL). The solvent was removed in vacuo to give 57.1 g (92%) of **14** as a colorless oil, which was used without purification in the next step. ¹H NMR (acetone-*d*₆) δ 4.23 (2H, dd, *J* = 7.1 Hz, 1.0 Hz), 6.10 (1H, dt, *J* = 16.0 Hz, 1.0 Hz), 6.31 (1H, dt, *J* = 7.1 Hz, 16.0 Hz), 7.32–7.39 (3H, m), 7.41–7.48 (2H, m). ¹³C NMR 100 MHz (acetone-*d*₆) δ 45.43, 88.00, 92.47, 115.02, 124.19, 129.71, 129.88, 132.79, 139.71.

Isopropyl (*S*)-(E)-2-Ethoxy-3-[4-(5-phenylpent-2-en-4-ynyloxy)phenyl]propanoate. A mixture of isopropyl (*S*)-2-ethoxy-3-(4-hydroxyphenyl)propanoate (47.14 g, 186.8 mmol), **14** (30.0 g, 169.8 mmol), potassium carbonate (35.21 g, 254.7 mmol), and potassium iodide (2.82 g, 17.0 mmol) in acetone (100 mL) was refluxed for 4–5 h. The solid was filtered off and the acetone removed in vacuo to yield an oil. The oil was dissolved in *tert*-butylmethyl ether (MTBE) (100 mL) and washed with 1 M NaOH (3 \times 50 mL) and saturated NaCl solution (50 mL). The organic phase was then dried over Na₂SO₄ and the solvent removed in vacuo after filtration to give 59.99 g (90%) of the title compound as a colorless oil, which was used without purification in the next step. ¹H NMR (CDCl₃) δ 1.15 (3H, d, *J* = 7 Hz), 1.16 (3H, t, *J* = 7 Hz), 1.22 (3H, d, *J* = 7 Hz), 2.94 (2H, d, *J* = 6.6 Hz), 3.35 (1H, m), 3.59 (1H, m), 3.94 (1H, t, *J* = 6.6 Hz), 4.59 (2H, dd, *J* = 5.3 Hz, 1.8 Hz), 4.98–5.07 (1H, m), 6.05 (1H, dt, *J* = 15.8 Hz, 1.8 Hz), 6.36 (1H, dt, *J* = 15.8 Hz, 5.3 Hz), 6.82 (2H, d, *J* = 9 Hz), 7.16 (2H, d, *J* = 9 Hz), 7.28–7.30 (3H, m), 7.41–7.43 (2H, m). ¹³C NMR 100 MHz (CDCl₃) δ 15.51, 22.23, 38.83, 66.48, 68.05,

68.75, 80.81, 87.55, 91.01, 112.66, 114.92, 123.54, 128.73, 130.12, 130.92, 131.93, 138.17, 157.50, 172.52.

(*S*)-(E)-2-Ethoxy-3-[4-(5-phenylpent-2-en-4-ynyloxy)phenyl]propanoic Acid, 6. A mixture of isopropyl (*S*)-(E)-2-ethoxy-3-[4-(5-phenylpent-2-en-4-ynyloxy)phenyl]propanoate (39.25 g, 100.0 mmol), aqueous 1M NaOH (150 mL), and ethanol (96%, 130 mL) was heated for 1–2 h to 70 °C with stirring. Most of the ethanol was then distilled off followed by the addition of saturated NaCl solution (150 mL). The basic water phase was washed with MTBE (2 \times 50 mL) at 50–55 °C. MTBE (50 mL) was added to the aqueous phase followed by addition of concentrated hydrochloric acid until pH 2. The organic phase was separated and the water phase extracted once more with MTBE (50 mL). The combined organic phases were dried over Na₂SO₄ and filtered, and the solvent removed in vacuo to give 33.99 g (97%) of **6** as an oil, which crystallized on standing. An analytical sample of **6** could be obtained by crystallization as the benzylamine salt in MTBE followed by liberation of the free acid. ¹H NMR (acetone-*d*₆) δ 1.10 (3H, t, *J* = 7 Hz), 2.90 (1H, dd, *J* = 14 Hz, 8 Hz), 3.01 (1H, dd, *J* = 14 Hz, 4 Hz), 3.38 (1H, dq, *J* = 7 Hz, 9 Hz), 3.63 (1H, dq, *J* = 7 Hz, 9 Hz), 4.04 (1H, dd, *J* = 8 Hz, 4 Hz), 4.69 (2H, dd, *J* = 5.3 Hz, 1.8 Hz), 6.14 (1H, dt, *J* = 16 Hz, 1.8 Hz), 6.43 (1H, dt, *J* = 16 Hz, 5.3 Hz), 6.90 (2H, d, *J* = 8.5 Hz), 7.21 (2H, d, *J* = 8.5 Hz), 7.36–7.40 (3H, m), 7.43–7.47 (2H, m). ¹³C NMR 100 MHz (acetone-*d*₆) δ 15.41, 38.77, 66.37, 68.09, 80.53, 88.03, 90.89, 112.38, 115.19, 124.01, 129.30, 129.39, 130.96, 131.32, 132.20, 139.66, 158.04, 173.38.

(*S*)-(E)-2-Ethoxy-3-[4-(5-phenylpent-2-en-4-ynyloxy)phenyl]propanoic Acid L-Arginine, 6-L-Arginine Salt. (*S*)-(E)-2-Ethoxy-3-[4-(5-phenylpent-2-en-4-ynyloxy)phenyl]propanoic acid, **6**, (35.04 g, 0.1 mol) was dissolved in 2-propanol (260 mL). The solution was heated to reflux and a hot (~70 °C) solution of L-arginine (17.42 g, 0.1 mol) dissolved in water (350 mL) was added dropwise with stirring. The solution was allowed to cool slowly to room temperature (the solution became opaque at ~65 °C and seeding might be necessary at this temperature in order to ensure a proper crystallization). The crystals formed were filtered off, washed with 2-propanol (2 \times 100 mL), and dried at 30–45 °C in vacuo to give 45.1 g (86%) of the title compound. Mp 195 °C (DSC). ee > 96% (CE). ESI-MS: 351 (MH⁺). ¹H NMR (DMSO-*d*₆) δ 0.99 (3H, t, *J* = 7 Hz), 1.50–1.81 (4H, m), 2.66 (1H, dd, *J* = 14 Hz, 9 Hz), 2.83 (1H, dd, *J* = 14 Hz, 4 Hz), 2.95–3.63 (10H, m), 4.65 (2H, d, *J* = 5.3 Hz), 6.14 (1H, d, *J* = 16 Hz), 6.41 (1H, dt, *J* = 16 Hz, 5.3 Hz), 6.84 (2H, d, *J* = 8.5 Hz), 7.14 (2H, d, *J* = 8.5 Hz), 7.36–7.41 (3H, m), 7.42–7.48 (2H, m), 7.90–8.30 (4H, br.s). ¹³C NMR 100 MHz (DMSO-*d*₆) δ 15.55, 24.88, 28.61, 38.78, 40.50, 53.76, 64.24, 67.35, 82.53, 87.86, 90.55, 111.78, 114.44, 122.68, 129.06, 130.41, 131.61, 132.53, 139.75, 156.41, 158.10, 172.52, 176.88. Anal. (C₂₂H₂₁O₄.C₆H₁₄N₄O₂) C, H, N.

Ethyl (*E*)-3-(4-Iodophenyl)but-2-enoate, 15. Sodium (5.52 g, 0.24 mol) was dissolved in ethanol (200 mL). A solution of triethyl phosphonoacetate (62.7 g, 0.28 mol) in ethanol (100 mL) was slowly added, the mixture stirred for 20 min, and a solution of 4-iodoacetophenone (49.21 g, 0.20 mol) in hot ethanol (200 mL) added. The reaction mixture was stirred at 80 °C for 66 h. The mixture was cooled and the ethanol evaporated. To the residue were added 1 N HCl (400 mL) and ethyl acetate (400 mL). The aqueous layer was separated and further extracted with ethyl acetate (2 \times 200 mL). The combined organic phases were washed with brine, dried (MgSO₄), filtered, and evaporated. The product was purified by column chromatography using heptane:ethyl ether (39:1) as eluent to give 58.2 g (92%) of the title compound. ¹H NMR (CDCl₃) δ 1.31 (3H, t, *J* = 7 Hz), 2.53 (3H, d, *J* = 1.1 Hz), 4.21

(2H, q, $J = 7$ Hz), 6.11 (1H, q, $J = 1.1$ Hz), 7.19 (2H, d, $J = 8$ Hz), 7.69 (2H, d, $J = 8$ Hz).

(E)-3-(4-Iodophenyl)but-2-en-1-ol, 16. Under an atmosphere of nitrogen, **15** (10.1 g, 32.0 mmol) was dissolved in dry THF (300 mL). The solution was cooled to -15 °C, and a 1 M solution of DIBAL-H in toluene (96.0 mL, 96.0 mmol) was added slowly. The mixture was slowly warmed to room temperature and stirred for 1 h. Methanol (50 mL) was carefully added, followed by 1 N HCl (500 mL), and the resulting mixture was extracted with ethyl acetate (3×500 mL). The combined organic extracts were washed with brine, dried (MgSO_4), and evaporated to give 8.8 g (100%) of the title compound as a white crystalline solid. $^1\text{H NMR}$ (DMSO) δ 1.38 (1H, t, $J = 5.3$ Hz), 2.04 (3H, d, $J = 1.1$ Hz), 4.35 (2H, t, $J = 5.6$ Hz), 5.93–6.00 (1H, m), 7.14 (2H, d, $J = 8.5$ Hz), 7.65 (2H, d, $J = 8.5$ Hz).

(E)-1-[4'-(4-Hydroxy-2-but-2-en-2-yl)biphenyl-4-yl]ethanone, 17. Tetrakis(triphenylphosphine)-palladium (0.46 g, 0.4 mmol, 4 mol %) was added, under nitrogen, to a stirred solution of **16** (2.74 g, 10.0 mmol) in DME (100 mL), and the solution stirred at room temperature for 10 min. Aqueous 2M sodium carbonate (30 mL, 60 mmol) was then added, and the mixture stirred for 10 min. Then 4-acetylphenylboronic acid (3.28 g, 20.0 mmol) was added, and the reaction mixture was heated to 65 °C for 18 h and at room temperature for another 3 days. The reaction mixture was diluted with 1N HCl (200 mL) and the products extracted into ethyl acetate (2×200 mL). The combined organic extracts were washed with brine, dried (MgSO_4), and evaporated to give the crude product. Purification by column chromatography using heptane:ethyl acetate (3:2) as eluent gave 2.0 g (75%) of the title compound as a off-white solid. $^1\text{H NMR}$ (CDCl_3) δ 2.12 (3H, s), 2.64 (3H, s), 4.41 (2H, d, $J = 6.8$ Hz), 6.07 (1H, m), 7.54 (2H, d, $J = 8.5$ Hz), 7.61 (2H, d, $J = 8.5$ Hz), 7.71 (2H, d, $J = 8.5$ Hz), 8.03 (2H, d, $J = 8.5$ Hz).

(E)-1-[4'-(4-(tert-Butyldimethylsilyloxy)but-2-en-2-yl)biphenyl-4-yl]ethanone, 18. To a suspension of **17** (1.1 g, 4.13 mmol) in methylene chloride (40 mL) were added under an atmosphere of nitrogen imidazole (0.42 g, 6.20 mmol) and *tert*-butyldimethylsilyl chloride (0.78 g, 5.15 mmol). The mixture was stirred at room temperature for 18 h. Methylene chloride (15 mL) was added and the reaction mixture was washed with water, sodium hydrogencarbonate solution and brine. The organic phase was dried (MgSO_4), filtered and concentrated in vacuo. The residue was purified by column chromatography using heptane:ethyl acetate (4:1) as eluent to give 1.36 g (87%) of the title compound as a white crystalline solid. Mp 100–106 °C. $^1\text{H NMR}$ (CDCl_3) δ 0.13 (6H, s), 0.97 (9H, s), 2.10 (3H, s), 2.65 (3H, s), 4.45 (2H, d, $J = 7$ Hz), 5.98 (1H, dt, $J = 5$ Hz, 1 Hz), 7.51 (2H, d, $J = 8$ Hz), 7.60 (2H, d, $J = 8$ Hz), 7.69 (2H, d, $J = 8$ Hz), 8.02 (2H, d, $J = 8$ Hz).

Ethyl (E,E)-3-(4'-(4-(tert-Butyldimethylsilyloxy)but-2-en-2-yl)biphenyl-4-yl)but-2-enoate. Sodium (0.42 g, 18.0 mmol) was added to ethanol (50 mL) at 20 °C and the reaction mixture was stirred until the metal had fully reacted. Triethyl phosphonoacetate (2.4 mL, 12.0 mmol) was added, and the mixture was stirred for 5 min. Then **18** (1.14 g, 3.0 mmol) was added to the stirred solution and the reaction was stirred at room temperature for 24 h. To the reaction mixture was added water and the product extracted with ethyl acetate (2×300 mL). The combined organic phases were washed with brine, dried (MgSO_4), filtered and concentrated in vacuo. The residue was purified by column chromatography using heptane:ethyl acetate (4:1) as eluent to give 1.13 g (81%) of the title compound. $^1\text{H NMR}$ (CDCl_3) δ 0.12 (6H, s), 0.92 (9H, s), 1.32 (3H, t, $J = 7$ Hz), 2.08 (3H, s), 2.62 (3H, s), 4.22 (2H, q, $J = 7$ Hz), 4.42 (2H, d, $J = 7$ Hz), 5.97 (1H, dt, $J = 5$ Hz, 1 Hz), 6.20 (1H, d, $J = 1$ Hz), 7.43–7.63 (8H, m).

(E,E)-3-(4'-(4-(tert-Butyldimethylsilyloxy)but-2-en-2-yl)biphenyl-4-yl)but-2-en-1-ol, 19. A 1M solution of DIBAL-H in toluene (7.3 mL, 7.3 mmol) was, under an atmosphere of nitrogen, added dropwise at -70 °C over 20 min to a stirred solution of ethyl (E,E)-3-(4'-(4-(tert-butylidimethylsilyloxy)but-2-en-2-yl)biphenyl-4-yl)but-2-enoate (1.13 g, 2.43 mmol) in dry

THF (25 mL). The mixture was stirred for 30 min at -70 °C followed by 2 h at room temperature. Ethanol (1 mL) was carefully added, followed by 1N HCl (50 mL) and the resulting mixture was extracted with ethyl acetate (2×50 mL). The combined organic extracts were washed with brine, dried (MgSO_4), and evaporated to give 1.02 g (99%) of the title compound. $^1\text{H NMR}$ (CDCl_3) δ 0.13 (6H, s), 0.96 (9H, s), 1.57 (1H, s), 2.07 (3H, s), 2.13 (3H, s), 4.37–4.46 (4H, m), 5.98 (1H, dt, $J = 5$ Hz, 1 Hz), 6.06 (1H, dt, $J = 5$ Hz, 1 Hz), 7.46–7.52 (4H, m), 7.53–7.61 (4H, m).

Ethyl (E,E)-(S)-3-{4-[3-(4'-(4-(tert-Butyldimethylsilyloxy)but-2-en-2-yl)biphenyl-4-yl)but-2-en-1-yloxy]phenyl}-2-ethoxypropanoate, 20. Under an atmosphere of nitrogen, azodicarboxylic dipiperidine (0.91 g, 3.62 mmol) was added at 0–5 °C to a stirred solution of tributylphosphine (0.89 mL, 3.62 mmol), ethyl (S)-2-ethoxy-3-(4-hydroxyphenyl)propanoate (0.60 g, 2.53 mmol) and **19** (1.02 g, 2.41 mmol) in dry THF (15 mL). The mixture was warmed to room temperature and stirred for 18 h. The resulting mixture was diluted with water and ethyl acetate, the aqueous layer collected and further extracted with ethyl acetate. The organic layers were combined, washed with brine, dried (MgSO_4), and evaporated. The crude product was then purified by column chromatography using heptane:ethyl acetate (4:1) as eluent to give 1.18 g (76%) of the title compound. $^1\text{H NMR}$ (CDCl_3) δ 0.13 (6H, s), 0.93 (9H, s), 1.18 (3H, t, $J = 7$ Hz), 1.23 (3H, t, $J = 7$ Hz), 2.07 (3H, s), 2.18 (3H, s), 2.95 (2H, d, $J = 7$ Hz), 3.31–3.42 (1H, m), 3.55–3.67 (1H, m), 3.98 (1H, t, $J = 7$ Hz), 4.17 (2H, q, $J = 7$ Hz), 4.42 (2H, d, $J = 6$ Hz), 4.73 (2H, d, $J = 6$ Hz), 5.95 (1H, t, $J = 5$ Hz), 6.12 (1H, t, $J = 5$ Hz), 6.88 (2H, d, $J = 8$ Hz), 7.18 (2H, d, $J = 8$ Hz), 7.45–7.60 (8H, m).

Ethyl (E,E)-(S)-3-{4-[3-(4'-(4-Hydroxybut-2-en-2-yl)biphenyl-4-yl)but-2-en-1-yloxy]phenyl}-2-ethoxypropanoate. A solution of **20** (1.18 g, 1.84 mmol) in dry THF was cooled on ice, and a 1.1 M solution of tetrabutylammonium fluoride in THF (1.93 mL, 2.12 mmol) was slowly added. The reaction mixture was stirred at room temperature for 3 h. The mixture was diluted with water and ethyl acetate, and the aqueous layer was collected and further extracted with ethyl acetate. The organic layers were combined, washed with brine, dried (MgSO_4), and evaporated to give 0.94 g (99%) of the title compound. $^1\text{H NMR}$ (CDCl_3) δ 1.18 (3H, t, $J = 7$ Hz), 1.22 (3H, t, $J = 7$ Hz), 2.12 (3H, s), 2.18 (3H, s), 2.96 (2H, d, $J = 7$ Hz), 3.30–3.42 (1H, m), 3.53–3.67 (1H, m), 3.98 (1H, t, $J = 7$ Hz), 4.17 (2H, q, $J = 7$ Hz), 4.40 (2H, d, $J = 7$ Hz), 4.74 (2H, d, $J = 7$ Hz), 6.04 (1H, dt, $J = 5$ Hz, 1 Hz), 6.12 (1H, dt, $J = 5$ Hz, 1 Hz), 6.88 (2H, d, $J = 8$ Hz), 7.18 (2H, d, $J = 8$ Hz), 7.45–7.62 (8H, m).

Ethyl (E,E)-(S,S)-3-{4-[3-(4'-(4-(2-Ethoxy-2-ethoxy-carbonyl-ethyl)phenoxy)but-2-en-2-yl)biphenyl-4-yl)but-2-en-1-yloxy]phenyl}-2-ethoxypropanoate. Under an atmosphere of nitrogen, azodicarboxylic dipiperidine (0.50 g, 1.89 mmol) was added at 0–5 °C to a stirred solution of tributylphosphine (0.37 mL, 1.89 mmol), ethyl (S)-2-ethoxy-3-(4-hydroxyphenyl)propanoate (0.32 g, 1.32 mmol), and ethyl (E,E)-(S)-3-{4-[3-(4'-(4-hydroxybut-2-en-2-yl)biphenyl-4-yl)but-2-en-1-yloxy]phenyl}-2-ethoxypropanoate (0.65 g, 1.26 mmol) in dry THF (15 mL). The mixture was warmed to room temperature and stirred for 18 h. The resulting mixture was diluted with water and ethyl acetate, and the aqueous layer was collected and further extracted with ethyl acetate. The organic layers were combined, washed with brine, dried (MgSO_4), and evaporated to give 580 mg (63%) of the title compound. $^1\text{H NMR}$ (CDCl_3) δ 1.17 (6H, t, $J = 7$ Hz), 1.22 (6H, t, $J = 7$ Hz), 2.16 (6H, s), 2.97 (4H, d, $J = 7$ Hz), 3.27–3.43 (2H, m), 3.52–3.69 (2H, m), 3.98 (2H, t, $J = 7$ Hz), 4.17 (4H, q, $J = 7$ Hz), 4.73 (4H, d, $J = 7$ Hz), 6.12 (2H, t, $J = 6$ Hz), 6.88 (4H, d, $J = 8$ Hz), 7.18 (4H, d, $J = 8$ Hz), 7.43–7.63 (8H, m).

(E,E)-(S,S)-3-{4-[3-(4'-(4-(4-(Ethoxy-2-carboxyethyl)phenoxy)but-2-en-2-yl)biphenyl-4-yl)but-2-en-1-yloxy]phenyl}-2-ethoxypropanoic Acid, 7. To a solution of ethyl (E,E)-(S,S)-3-{4-[3-(4'-(4-(2-ethoxy-2-ethoxycarbonyl)ethyl)phenoxy)but-2-en-2-yl)biphenyl-4-yl)but-2-en-1-yloxy]phenyl}-

2-ethoxypropanoate (367 mg, 0.5 mmol) in ethanol (10 mL) was added 1N sodium hydroxide (2 mL). The reaction mixture was stirred at room temperature for 18 h and at 60 °C for 1 h. The resulting mixture was diluted with water and ethyl acetate, and the aqueous layer was collected and further extracted with ethyl acetate (3 × 10 mL). The organic layers were combined, washed with brine, dried (MgSO₄) and evaporated to give 180 mg (53%) of the title compound. ee > 99% (CE). ¹H NMR (CDCl₃ + 1 dr. DMSO) δ 1.15 (6H, t, *J* = 7 Hz), 2.90–3.80 (4H, m), 3.30–3.42 (2H, m), 3.60–3.71 (2H, m), 3.95 (2H, dd, *J* = 5 Hz, 5 Hz), 4.73 (4H, d, *J* = 7 Hz), 6.11 (2H, t, *J* = 5 Hz), 6.88 (4H, d, *J* = 8 Hz), 7.21 (4H, d, *J* = 8 Hz), 7.51 (4H, d, *J* = 8 Hz), 7.57 (4H, d, *J* = 8 Hz). Mp 159–162.5 °C. Anal. (C₄₂H₄₆O₈) C, H, N.

(*E,E*)-5-[4-(5-Hydroxypent-3-en-1-ynyl)phenyl]pent-2-en-4-yn-1-ol, 21a. To a solution of 1,4-diiodobenzene (10.57 g, 32.0 mmol) in diisopropylamine (120 mL) under a nitrogen atmosphere were added copper(I) iodide (640 mg, 3.3 mmol) and tetrakis(triphenylphosphine)palladium (640 mg, 0.55 mmol). After the mixture had stirred for 1 h, a solution of 2-penten-4-yn-1-ol (10.5 g, 128.1 mmol) in diisopropylamine (60 mL) was added. After stirring under nitrogen at 60 °C for 2 h, the reaction mixture was cooled to room temperature and filtered through Celite. The filtrate was washed with ethyl acetate (50 mL) and evaporated to dryness. The product was purified by column chromatography using methylene chloride: THF (80:1) as eluent to give the crude product. The crude product was washed with ether (2 × 100 mL) giving the title compound in 8.35 g (100%) yield. ¹H NMR (DMSO) δ 4.10 (4H, m), 5.01 (2H, t, *J* = 7 Hz), 5.95 (2H, dt, *J* = 15 Hz, 2 Hz), 6.48 (2H, dt, *J* = 15 Hz, 5 Hz), 7.44 (4H, s).

(*E,E*)-5-[3-(5-Hydroxypent-3-en-1-ynyl)phenyl]pent-2-en-4-yn-1-ol, 21b. The title compound was synthesized in 6.25 g (86.5%) yield as described above for **21a**, using 1,3-diiodobenzene. ¹H NMR (DMSO) δ 4.09 (4H, m), 5.02 (2H, t, *J* = 7 Hz), 5.95 (2H, dt, *J* = 15 Hz, 2 Hz), 6.38 (2H, dt, *J* = 15 Hz, 5 Hz), 7.35–7.50 (4H, m).

Isopropyl (*E,E*)-(S,S)-2-Ethoxy-3-[4-[5-(4-[5-[4-(2-ethoxy-2-isopropoxycarbonyl)ethyl]phenoxy]pent-3-en-1-ynyl)-phenyl]pent-2-en-4-ynyloxy]phenyl]propanoate. Under an atmosphere of nitrogen, azodicarboxylic dipiperidide (21.4 g, 84.8 mmol) was added at room temperature to a stirred solution of tributylphosphine (17.1 g, 84.8 mmol), isopropyl (S)-2-ethoxy-3-(4-hydroxyphenyl)propanoate (21.4 g, 84.8 mmol), and **21a** (7.6 g, 30.0 mmol) in dry THF (300 mL). After 1 h water (100 mL) was added and the mixture was extracted with methylene chloride (3 × 100 mL). The combined extracts were dried and concentrated in vacuo, and the crude product was purified by column chromatography using methylene chloride: THF (20:1) as eluent to give 14.75 g (70%) of the title compound. ¹H NMR (CDCl₃) δ 1.18 (6H, t, *J* = 7 Hz), 1.23 (12H, t, *J* = 7 Hz), 2.95 (4H, d, *J* = 7 Hz), 3.30–3.43 (2H, m), 3.55–3.67 (2H, m), 3.95 (2H, t, *J* = 7 Hz), 4.63 (4H, dd, *J* = 7 Hz, 2 Hz), 5.05 (2H, m), 6.07 (2H, dt, *J* = 15 Hz, 2 Hz), 6.39 (2H, dt, *J* = 15 Hz, 5 Hz), 6.85 (4H, d, *J* = 8 Hz), 7.17 (4H, d, *J* = 8 Hz), 7.27 (4H, s), 7.37 (4H, s).

Isopropyl (*E,E*)-(S,S)-2-Ethoxy-3-[4-[5-(3-[5-[4-(2-ethoxy-2-isopropoxycarbonyl)ethyl]phenoxy]pent-3-en-1-ynyl)-phenyl]pent-2-en-4-ynyloxy]phenyl]propanoate. The title compound was synthesized as described above in 7.57 g (40%) yield using **21b**. ¹H NMR (CDCl₃) δ 1.17 (6H, t, *J* = 7 Hz), 1.23 (12H, d, *J* = 7 Hz), 2.95 (4H, d, *J* = 7 Hz), 3.30–3.41 (2H, m), 3.55–3.66 (2H, m), 3.95 (2H, t, *J* = 7 Hz), 4.62 (4H, dd, *J* = 2 Hz, 7 Hz), 5.00–5.10 (2H, m), 6.05 (2H, dt, *J* = 15 Hz, 2 Hz), 6.40 (2H, dt, *J* = 15 Hz, 5 Hz), 6.84 (4H, d, *J* = 8 Hz), 7.18 (4H, d, *J* = 8 Hz), 7.22–7.38 (3H, m), 7.50 (1H, s).

(*E,E*)-(S,S)-3-[4-[5-(4-[5-[4-(2-Carboxy-2-ethoxyethyl)-phenoxy]pent-3-en-1-ynyl]phenyl]pent-2-en-4-ynyloxy]phenyl]-2-ethoxypropanoic Acid, 8a. To a solution of isopropyl (*E,E*)-(S,S)-2-ethoxy-3-[4-[5-(4-[5-[4-(2-ethoxy-2-isopropoxycarbonyl)ethyl]phenoxy]pent-3-en-1-ynyl)-phenyl]pent-2-en-4-ynyloxy]phenyl]propanoate (14.75 g, 20.9 mmol) in ethanol (590 mL) was added 1 N sodium hydroxide (85 mL). After the reaction mixture was stirred at 80 °C for 1 h, the

reaction mixture was concentrated in vacuo, and water and 1 N hydrochloric acid to pH 1 were added. The product was extracted with ether (3 × 300 mL), and the combined organic phases were dried (MgSO₄), filtered, and concentrated in vacuo to give the title compound as a crystalline product in 8.0 g (62%) yield. ee > 92% (CE). ¹H NMR (CDCl₃) δ 1.19 (6H, t, *J* = 7 Hz), 2.90–3.14 (4H, m), 3.42–3.66 (4H, m), 4.06 (2H, m), 4.62 (4H, dd, *J* = 7 Hz, 2 Hz), 6.07 (2H, dt, *J* = 15 Hz, 2 Hz), 6.39 (2H, dt, *J* = 15 Hz, 5 Hz), 6.84 (4H, d, *J* = 8 Hz), 7.15 (4H, d, *J* = 8 Hz), 7.35 (4H, s). Mp 156–158 °C. Anal. (C₃₈H₃₈O₈) C, H, N.

(*E,E*)-(S,S)-3-[4-[5-(3-[5-[4-(2-Carboxy-2-ethoxyethyl)-phenoxy]pent-3-en-1-ynyl]phenyl]pent-2-en-4-ynyloxy]phenyl]-2-ethoxypropanoic Acid, 8b. The title compound was synthesized as described for compound **8a** above in 6.52 g (99%) yield. ee > 96% (CE). ¹H NMR (CDCl₃) δ 1.18 (6H, t, *J* = 7 Hz), 2.88–3.15 (4H, m), 3.33–3.70 (4H, m), 4.05 (2H, m), 4.62 (4H, dd, *J* = 7 Hz, 2 Hz), 6.05 (2H, dt, *J* = 15 Hz, 2 Hz), 6.38 (2H, dt, *J* = 15 Hz, 5 Hz), 6.85 (4H, d, *J* = 8 Hz), 7.17 (4H, d, *J* = 8 Hz), 7.23–7.40 (3H, m), 7.50 (1H, s). Mp 76–79 °C. Anal. (C₃₈H₃₈O₈) C, H, N.

Chiral Analysis. The CE analyses were performed on a HP3DCE capillary electrophoresis instrument (Agilent, Waldborn, Germany) equipped with an auto sampler, a capillary cartridge, a high-voltage power supply, a diode array detector, electrodes, and a hydrostatic injection system. The electrophoretic data system was the HP Chemstation software, and the data were collected with a frequency of 10 Hz. The CE separations were carried out with untreated fused-silica capillaries from Agilent with the following dimensions: 80.5 cm total length with 72.0 cm effective length, 50 μm inner diameter, and extended light path with an inner diameter of 150 μm at the detector window. The electrolyte was prepared by dissolving 3.0% (w/v) sulfobutyl ether-β-cyclodextrin (Advasep 4, Cydex, Inc., Overland Park, KS) and 0.50% (w/v) dimethyl-β-cyclodextrin (Agilent, Waldborn, Germany) both in 50 mM borate buffer pH 9.3 (Agilent) followed by filtering through a 0.45 μm polypropylene filter. To this solution was added 5% (v/v) acetonitrile to give the final electrolyte. The electrophoresis was carried out in normal polarity mode. The electrophoretic conditions were as follows: voltage, 21 kV; current, 50 μA; capillary temperature controlled at 25 °C; injection was 50 mbar for 4.0 s; detection, UV at 205 nm with reference of 380 nm. The sample concentration was 0.05 mg/mL in 1/5 acetonitrile/5 mM borate buffer pH 9.3. The capillary was conditioned with 0.1 N NaOH for 20 min daily and flushed with 0.1 N NaOH (3 min), water (2 min), and electrolyte (3 min) between each run.

Modeling. The docking experiments were performed with FlexX version 1.10.0^{30–33} with assignment of formal charges and DrugScore³⁴ as docking method. Consensus scoring was applied on the obtained solutions.³⁵ FlexX was used with the Sybyl6.8 interface.³⁶

In Vitro Transactivation. The PPAR transactivation assay has been described previously.¹³ Briefly, the ligand binding domains of the three human PPAR receptor subtypes as well as that of rat PPARα (amino acids 167–469 (end)) were fused to the DNA binding domain (amino acids 1–147) of the yeast transcription factor Gal4. HEK293 cells were transiently transfected with an expression vector for the respective PPAR chimera along with a reporter construct containing five copies of the Gal4 DNA binding site driving expression of a luciferase reporter gene. All compounds were dissolved in DMSO and diluted 1:1000 upon addition to the cells. Compounds were tested in five concentrations ranging from 0.01 to 30 μM. Cells were treated with compound for 24 h followed by luciferase assay. EC₅₀ values were calculated via nonlinear regression using GraphPad PRISM 3.02 (GraphPad Software, San Diego, CA). The results were expressed as means ± SD.

Pharmacokinetics. The procedure has previously been described in detail.¹³ Briefly, the compounds were dosed po and iv to male SD rats. The compounds were dissolved in 5% ethanol, 10% HPCD, and phosphate buffer; pH 7.5–8.0. Blood

samples were collected in EDTA tubes. Each data point represents one animal.

Plasma samples were analyzed by high turbulence liquid chromatography (HTLC) combined with tandem mass spectrometry (MS/MS).

In Vivo Model. The model has earlier been published in detail.¹³ Briefly, 14 weeks old C57BL/KsBom-db/db male mice ($n = 6$ per dose) were dosed by gavage, with a suspension of compound in 0.2% CMC + 0.4% Tween-80 in saline for 10 days. After 7 days of treatment, nonfasted blood samples were drawn and analyzed for full blood glucose and plasma triglycerides. On day 9 of treatment an oral glucose tolerance test (OGTT) was performed on overnight fasted animals. Blood samples from the tail vein were drawn before and at 30, 60, and 120 min after the glucose dosing (3 g/kg).

Statistics: ED₅₀ values were calculated via nonlinear regression using GraphPad PRISM 3.02 (GraphPad Software, San Diego, CA). The results were expressed as means \pm SEM. Differences between two groups were evaluated by one-way ANOVA and Dunett's multiple comparison test: * $P < 0.05$, ** $P < 0.01$. P values less than 0.05 were considered significant.

Percent reduction was calculated using the equation: $((C_v - C_i)/C_v) \times 100$, where C_v was the plasma concentration in the vehicle treated group, C_i the plasma concentration in the compound treated group.

Macromolecular Crystallography. Ligand binding domain (LBD, amino acids C₁₆₅ - Stop) PPAR γ was expressed, purified, and crystallized according to Ebdrup et al. (2003).¹⁴ The crystal space group and cell parameters obtained are found in Table X+1, Supporting Information. A crystal was transferred to a solution containing 48% polyethylene glycol 4000, 0.15 M Tris-HCl pH 8.0, and concentrated 7 and was left soaking for 7 days. The crystal was thereafter flash-frozen in liquid nitrogen and mounted on the goniostat in a nitrogen gas-stream at 100 K. Crystallographic data were collected at beamline I711, the MAX-laboratory, Sweden,³⁷ using a marCD system, and the data set was evaluated by the XDS program package.³⁸ The structure was subsequently refined by, first, the CNX program system³⁹ and, in later stages, by Refmac⁴⁰ of the CCP4 program system.⁴¹ Input model was the PPAR γ coordinates generated by Sauerberg et al. (2002),¹³ PDB code 1KNU. Introduction of 7 and corrections to the model according to electron density maps were made with use of the Quanta program.⁴² The program Xplo2D⁴³ was used for creation of ligand Parameter and Topology files used by the CNX program. According to refinement statistics and electron density maps, the occupancy of the ligand in the crystal was around 0.75. For data collection, refinement, and model statistics, see Supporting Information Table X+1. The coordinates of the 7/PPAR γ structure have been deposited in the Brookhaven Protein Data Bank.

Acknowledgment. The technical assistance from M. A. Zundel, B. Rosenberg, A. Bergholdt, V. Weil, B. Bentzen, S. J. Mozer, A. Ryager, F. G. Gundertofte, R. Burgdorf, N. Steffensen, L. Priskorn, H. Bach, A. Heerwagen, A. Zeneca, K. M. Klausen, C. Christensen, K. Pedersen, O. Larsson, S. von Eyben, P. S. Klifforth, and A. Ravn is highly appreciated.

Supporting Information Available: Table of interactions between 7 and the amino acids of the LBD-PPAR γ receptor protein (Table X). Table of data collection, refinement and model statistics (Table X+1). This material is available free of charge via the Internet at <http://pubs.acs.org>.

References

- Porte, D., Jr.; Schwartz, M. W. Diabetes complications: Why is Glucose Potentially Toxic? *Science* **1996**, *27*, 699–700.
- Chilcott, J.; Tappenden, P.; Jones, M. L.; Wright, J. P. A systematic Review of the Clinical Effectiveness of Pioglitazone in the treatment of type 2 Diabetes Mellitus. *Clin. Ther.* **2001**, *23*, 1792–1823.
- Boyle, P. J.; King, A. B.; Olansky, L.; Marchetti, A.; Lau, H.; Magar, R.; Martin, J. Effects of Pioglitazone and Rosiglitazone on the Blood Lipid Levels and Glycemic Control in Patients with Type 2 Diabetes Mellitus: A Retrospective Review of Randomly Selected Medical Records. *Clin. Ther.* **2002**, *24*, 3, 378–396.
- Staels, B.; Dallongeville, J.; Auwerx, J.; Schoonjans, K.; Leitersdorf, E.; Fruchart, J.-C. Mechanism of action of fibrates on lipid and lipoprotein metabolism. *Circulation* **1998**, *98*, 2088–2093.
- Oliver, W. R.; Shenk, J. L.; Snaith, M. R.; Russell, C. S.; Plunket, K. D.; Bodkin, N. L.; Lewis, M. C.; Winegar, D. A.; Sznajdman, M. L.; Lambert, M. H.; Xu, H. E.; Sternbach, D. D.; Kliever, S. A.; Hansen, B. C.; Willson, T. M. A selective peroxisome proliferator-activated receptor δ agonist promotes reverse cholesterol transport. *Proc. Natl. Acad. Sci. U.S.A.* **2001**, *98*, 5306–5311.
- Kliwer, S. A.; Umesono, K.; Noonan, D. J.; Heyman, R. A.; Evans, R. M. Convergence of 9-cis retinoic acid and peroxisome proliferator signaling pathways through heterodimer formation of their receptors. *Nature* **1992**, *358*, 771–774.
- Strand, J.; Sandeman, D.; Skovsted, B.; Edsberg, B. Müller, P. Ragaglitazar (NNC 61–0029, (–) DRF 2725): The efficacy and Safety of the Novel Dual PPAR α and PPAR γ Agonist in Patients with Type 2 Diabetes. *Diabetes* **2002**, *51*, suppl. 2, A144.
- Cronet, P.; Petersen, J. F. W.; Folmer, R.; Blomberg, N.; Sjöblom, K.; Karlsson, U.; Lindstedt, E.-L.; Bamberg, K.; Structure of the PPAR α and γ ligand binding domain in complex with AZ 242: Ligand selectivity and Agonist Activation in the PPAR family. *Structure* **2001**, *9*, 699–706.
- Etgen, G. J.; Oldham, B. A.; Johnson, W. T.; Broderick, C. L.; Montrose, C. R.; Brozinick, J. T.; Misener, E. A.; Bean, J. S.; Bensch, W. R.; Brooks, D. A.; Shuker, A. J.; Rito, C. A.; McCarthy, J. R.; Ardecky, R. A.; Tyhonas, J. S.; Dana, S. L.; Bilakovic, J. M.; Paterniti, J. R., Jr.; Ogilvie, K. M.; Liu, S.; Kauffman, R. F. A Tailored Therapy for the Metabolic Syndrome, The Dual Peroxisome Proliferator-Activated Receptor α/γ Agonist LY465608 Ameliorates Insulin Resistance and Diabetes Hyperglycemia While Improving Cardiovascular Risk Factors in Preclinical Models. *Diabetes* **2002**, *51*, 1083–1087.
- Lewis, M. C.; Winegar, D. A.; Bodkin, N. L.; Hansen, B. C.; Oliver, W. R. Improved Insulin Sensitivity and Dyslipidemia Following Oral Administration of Combination PPAR γ/α and PPAR δ Agonist in Obese Rhesus Monkeys. *Diabetes* **2002**, *51*, suppl. 2, A140.
- Lewis, M. C.; Wilson, J. G.; Franklin, M. C.; Brown, J. G.; Strole, C. A.; Oliver, W. R.; Winegar, D. A. Co-Administration of PPAR γ , α and δ Agonist, improves Efficacy Relative to PPAR γ Agonist Alone in ZDF rats. *Diabetes* **2002**, *51*, suppl. 2, A140.
- Mogensen, J. P.; Jeppesen, L.; Bury, P. S.; Pettersson, I.; Fleckner, J.; Nehlin, J.; Frederiksen, K. S.; Albreksten, T.; Din, N.; Mortensen, S. B.; Svensson, L. A.; Wassermann, K.; Wulff, E. M.; Ynddal, L.; Sauerberg, P. Design and synthesis of novel PPAR $\alpha/\gamma/\delta$ triple activators using a known PPAR α/γ dual activator as structural template. *Bioorg. Med. Chem. Lett.* **2003**, *13*, 257–260.
- Sauerberg, P.; Pettersson, I.; Jeppesen, L.; Bury, P. S.; Mogensen, J. P.; Wassermann, K.; Brand, C. L.; Sturis, J.; Wöldike, H. F.; Fleckner, J.; Andersen, A.-S. T.; Mortensen, S. B.; Svensson, L. A.; Rasmussen, H. B.; Lehmann, S. V.; Polivka, Z.; Sindelar, K.; Panajotova, V.; Ynddal, L.; Wulff, E. M. Novel tricyclic- α -alkoxyphenylpropionic Acids: Dual PPAR α/γ Agonists with Hypolipidemic and Antidiabetic Activity. *J. Med. Chem.* **2002**, *45*, 789–804.
- Ebdrup, S.; Pettersson, I.; Rasmussen, H. B.; Deussen, H.-J.; Jensen, A. F.; Mortensen, S. B.; Fleckner, J.; Pridal, L.; Nygaard, L.; Sauerberg, P. Synthesis, and Biological and Structural Characterization of the Dual Acting PPAR α/γ Agonist Ragaglitazar. *J. Med. Chem.* **2003**, *46*, 1306–1317.
- Allen, C. F. H.; Edens, C. O., Jr. Phenylpropargylaldehyde. *Organic Syntheses*; Wiley: New York, 1955; Collect. Vol. III, pp 731–733.
- Krause, N. Synthesis of Allenes by 1,6-Addition of Organocuprates to Polarized Enynes. *Chem. Ber.* **1990**, *123*, 2173–2180.
- Takeuchi, R.; Tanabe, K.; Tanaka, S. Stereodivergent Synthesis of (E)- and (Z)-2-Alken-4-yn-1-ols from 2-Propynoic Acid: A Practical Route via 2-Alken-4-ynoates. *J. Org. Chem.* **2000**, *65*, 1558–1561.
- Taylor, E. C. Iminium Salts in Organic Chemistry. In *Advances in Organic Chemistry: Methods and Results*, Ed.; John Wiley & Sons: New York, 1979.
- Willson, T. M.; Cobb, J. E.; Cowan, D. J.; Wiethe, R. W.; Correa, I. D.; Prakash, S. R.; Beck, K. D.; Moore, L. B.; Kliever, S. A.; Lehmann, J. M. The Structure–Activity Relationship between Peroxisome Proliferator-Activated Receptor γ Agonism and the Antihyperglycemic Activity of Thiazolidinediones. *J. Med. Chem.* **1996**, *39*, 665–668.
- Halazy, S. G-protein coupled receptor bivalent ligands and drug design. *Exp. Opin. Ther. Pat.* **1999**, *9*, 431–446.

- (21) Christopoulos, A.; Grant, M. K. O.; Ayoubzadeh, N.; Kim, O. N.; Sauerberg, P.; Jeppesen, L.; El-Fakahany, E. E. Synthesis and Pharmacological Evaluation of Dimeric Muscarinic Acetylcholine Receptor Agonists. *J. Pharmacol. Exp. Ther.* **2001**, *298*, 1260–1268.
- (22) Nolte, R. T.; Wisely, G. B.; Westin, S.; Cobb, J. E.; Lambert, M. H.; Kurokawa, R.; Rosenfeld, M. G.; Willson, T. M.; Glass, C. K.; and Milburn, M. V. Ligand binding and co-activator assembly of the peroxisome proliferator-activated receptor-gamma. *Nature* **1998**, *395*, 137–143.
- (23) Uppenberg, J.; Svensson, C.; Jaki, M.; Bertilsson, G.; Jendeborg, L.; Berkenstam, A. Crystal Structure of the Ligand Binding Domain of the Human Nuclear Receptor PPAR γ . *J. Biol. Chem.* **1998**, *273*, 31108–31112.
- (24) Lipinski, C. A.; Lombardo, F.; Dominy, B. W.; Feeney, P. J. Experimental and computational approaches to estimate solubility and permeability in drug discovery and development settings. *Adv. Drug Delivery Rev.* **1997**, *23*, 3–25.
- (25) Veber, D. F.; Johnson, S. R.; Cheng, H.-Y.; Smith, B. R.; Ward, K. W.; Kopple, K. D. Molecular Properties That Influence the Oral Bioavailability of Drug candidates. *J. Med. Chem.* **2002**, *45*, 2615–2623.
- (26) Faber, K. N.; Müller, M.; Jansen, P. L. M. Drug transport proteins in the liver. *Adv. Drug Delivery Rev.* **2003**, *55*, 107–124.
- (27) Gampe, R. T.; Montana, V. G.; Lambert, M. H.; Miller, A. B.; Bledsoe, R. K.; Milburn, M. V.; Kliewer, S. A.; Willson, T. M.; Xu, H. E. Asymmetry in the PPAR γ /RXR α Crystal Structure Reveals the Molecular Basis of Heterodimerization among Nuclear Receptors. *Mol. Cell* **2000**, *5*, 545–555.
- (28) Oberfield, J. L.; Collins, J. L.; Holmes, C. P.; Goreham, D. M.; Cooper, J. P.; Cobb, J. E.; Lenhard, J. M.; Hull-Ryde, E. A.; Mohr, C. P.; Blanchard, S. G.; Parks, D. J.; Moore, L. B.; Lehmann, J. M.; Plunket, K.; Miller, A. B.; Milburn, M. V.; Kliewer, S. A.; Willson, T. M. A peroxisome proliferator-activated receptor γ ligand inhibits adipocyte differentiation. *Proc. Natl. Acad. Sci. U.S.A.* **1999**, *96*, 6102–6106.
- (29) Several other dimeric ligands have subsequently shown potent PPAR activity. Sauerberg et al. Unpublished.
- (30) Rarey, M.; Kramer, B.; Lengauer, T.; Klebe, G. A Fast Docking Method using an Incremental Construction Algorithm *J. Mol. Biol.* **1996**, *261*, 470–489.
- (31) Kramer, B.; Rarey, M.; Lengauer, L. Evaluation of the FlexX incremental construction algorithm for protein–ligand docking. *Proteins: Struct. Funct. Genet.* **1999**, *37*, 228–241.
- (32) Rarey, M.; Wefing, S.; Lengauer, T. Placement of medium-sized molecular fragments into active sites of proteins. *J. Comput.-Aided Mol. Design* **1996**, *10*, 41–54.
- (33) Rarey, M.; Kramer, B.; Lengauer, T. Multiple automatic base selection: Protein–ligand docking based on incremental construction without manual intervention. *J. Comput.-Aided Mol. Des.* **1997**, *11*, 369–384.
- (34) Sotriffer, C. A.; Gohlke, H.; Klebe, G. Docking into Knowledge-Based Potential Fields: A Comparative Evaluation of DrugScore. *J. Med. Chem.* **2002**, *45*, 1967–1970.
- (35) Clark, R. D.; Strizhev, A.; Leonard, J. M.; Blake, J. F.; Matthew, J. B. Consensus scoring for ligand/protein interactions. *J. Mol. Graph. Mod.* **2002**, *20*, 281–295.
- (36) SYBYL 6.8 Tripos Inc., 1699 South Hanley Rd., St. Louis, MO 63144.
- (37) Cerenius, Y.; Ståhl, K.; Svensson, L. A.; Ursby, T.; Oskarsson, Å.; Albertsson, J.; Liljas, A. The crystallography beamline I711 at MAX II. *J. Synchrotron Rad.* **2000**, *7*, 203–208.
- (38) Kabsch, W. Automatic processing of rotation diffraction data from crystals of initially unknown symmetry and cell constants. *J. Appl. Crystallogr.* **1993**, *26*, 795–800.
- (39) Brünger, A. T.; Krukowski, A.; Erickson, J. W. Slow-cooling protocols for crystallographic refinement by simulated annealing. *Acta Crystallogr. Sect. A* **1990**, *46*, 585–593.
- (40) Murshudov, G. N.; Vagin, A. A.; Dodson, E. J. Refinement of macromolecular structures by the maximum-likelihood method. *Acta Crystallogr. Sect. D* **1997**, *53*, 240–255.
- (41) Bailey, S. The ccp4 suite – programs for protein crystallography. *Acta Crystallogr. Sect. D* **1994**, *50*, 760–763.
- (42) Oldfield, T. J.; Hubbard, R. E. Analysis of c-alpha geometry in protein structures. *Proteins* **1994**, *18*, 324–337.
- (43) Kleywegt, G. J.; Jones, T. A. Databases in protein Crystallography. *Acta Crystallogr. Sect. D* **1998**, *54*, 1119–1131.

JM0309046